

New approach to synthesis of nitronyl and imino nitroxides based on S_N^H methodology

Evgeny V. Tretyakov,^{a*} Irina A. Utepova,^b Mikhail V. Varaksin,^b Svyatoslav E. Tolstikov,^a Galina V. Romanenko,^a Artem S. Bogomyakov,^a Dmitry V. Stass,^c Victor I. Ovcharenko,^a and Oleg N. Chupakhin^{b,d}

^aInternational Tomography Center, Siberian Branch of the Russian Academy of Sciences,
3a Institutskaya str., 630090 Novosibirsk, Russian Federation

^bDepartment of Organic Chemistry, Ural Federal University, 19 Mira str.,
Ekaterinburg, 620002, Russian Federation

^cInstitute of Chemical Kinetics and Combustion, Siberian Branch of the Russian Academy of Sciences, 3 Institutskaya str., 630090, Novosibirsk, Russian Federation

^dInstitute of Organic Synthesis, Ural Branch of the Russian Academy of Sciences,
20 S. Kovalevskoy str., Ekaterinburg, 620990, Russian Federation

E-mail: tev@tomo.nsc.ru

Dedicated to Professor Usein M. Dzhemilev on the occasion of his 65th birthday

Abstract

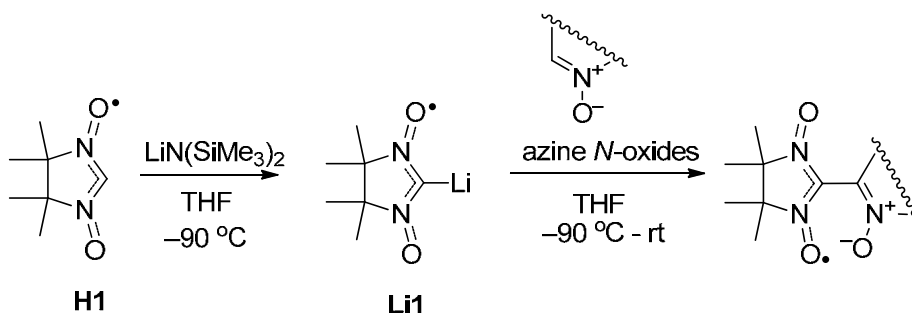
It is shown that S_N^H approach opens new possibilities in the synthesis of polyfunctional nitronyl and imino nitroxides. It is found that the interaction of 4,4,5,5-tetramethyl-4,5-dihydro-1H-imidazol-3-oxide-1-oxyl lithium salt **Li1** with 3,6-diaryl-1,2,4-triazines leads to formation of the corresponding triazines bearing nitronyl nitroxide or imino nitroxide substituent at position 5 of the heterocycle. The reaction of **Li1** with pyridazine-N-oxide gives rise to nitroxide with buten-3-ynyl substituent **5**. Spin-labeled **5** could be readily transformed by the use of 1,3-dipolar and nucleophilic addition reactions, as well as oxidative coupling, that gives a large group of new paramagnets: 2-(1H-pyrazol-5-yl)vinyl-, 2-ethynylcyclopropyl-, 2-(3-(ethoxycarbonyl) isoxazol-5-yl)vinyl-, 1-(pyrrolidin-1-yl)but-3-ynyl-substituted nitronyl nitroxide and a diradical – 2,2'-((1E,7E)-octa-1,7-dien-3,5-diyne-1,8-diyl)bis(4,4,5,5-tetramethyl-4,5-dihydro-1H-imidazol-3-oxide-1-oxyl). The new nitroxides were characterized by X-ray single crystal data, ESR and static magnetic susceptibility measurements.

Keywords: Nitronyl nitroxides, imino nitroxides, S_N^H reactions, X-ray diffraction study, ESR spectra

Introduction

The increasing application of polyfunctional nitronyl nitroxides (NNs)¹ in the field of molecular magnetism stimulates the development of the chemistry of these compounds.² The latter includes developing new methods for the targeted synthesis of kinetically stable NNs and methods for their isolation in the form of individual phases, as well as searching for new and general approaches to the synthesis of polyfunctional NNs. A possible pathway involves using a certain synthone that preserves the paramagnetic fragment. NN **H1** is such a candidate synthone. Under the action of $\text{KO}^\text{t}\text{Bu}$, LiNPr_2 , or $\text{LiN}(\text{SiMe}_3)_2$ it forms stable paramagnetic organometallic derivatives **M1** $\{\text{p}K_\text{a}(\text{H1}) \approx 21.9^3\}$, which upon further reaction with electrophilic reagents yield the products of $\text{C}(2)$ -functionalization.⁴

In the course of our study of nucleophilic substitution of hydrogen atom in π -deficient azine- N -oxides under the action of organolithium derivative **Li1** we found an efficient method for production of hetaryl-substituted NNs based on $\text{S}_\text{N}^\text{H}$ methodology (Scheme 1).⁵



Scheme 1

We note that in the reaction of different azine- N -oxides (pyridine- N -oxide, 2,2'-bipyridyl- N -oxide, quinoline- N -oxide, isoquinoline- N -oxide, phthalazine- N -oxide, pyrazine- N -oxide, quinoxaline- N -oxide, quinoxaline-1,4-dioxide, 3,6-diphenyl-1,2,4-triazine-4-oxide) the N -oxide group was preserved in the aromatization of the intermediate σ^H -adducts. These reactions were the first examples of a new general strategy for the synthesis of NNs. This work seeks new approaches to the synthesis of hitherto inaccessible polyfunctional NNs using **Li1** as the starting compound.

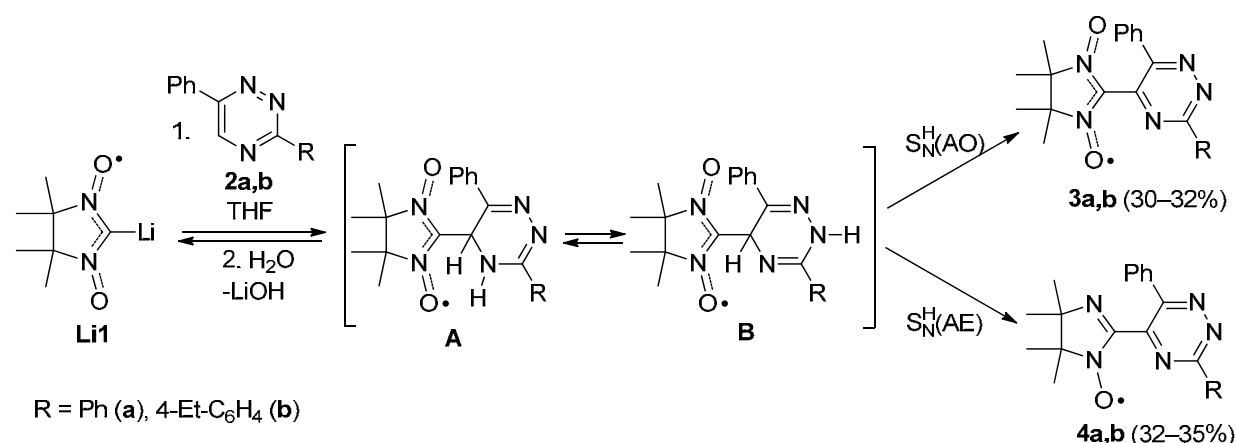
Results and Discussion

Syntheses

According to generally accepted views the $\text{S}_\text{N}^\text{H}$ reactions occur in two stages.⁶ At the first stage a nucleophilic fragment adds to a compound having electron-withdrawing substituents forming a σ^H -adduct, and at the second stage these intermediates aromatize into the corresponding $\text{S}_\text{N}^\text{H}$

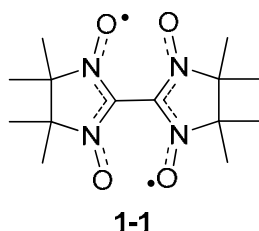
products. Two types of aromatization exist, viz., oxidative and eliminative, thus leading to two types of S_N^H reactions: S_N^H (AO) and S_N^H (AE). The first process requires an oxidizing reagent. The elimination-type aromatization requires the presence of an auxiliary group with propensity to anionic stabilization in the (hetero)aromatic substrate or in the nucleophilic moiety ("vicarious" nucleophilic substitution⁷).

We found that interaction of highly electrophilic derivatives of 1,2,4-triazine (3,6-diphenyl-1,2,4-triazine **2a** or 3-(4-ethylphenyl)-6-phenyl-1,2,4-triazine **2b**) with **Li1** results in formation of the products of S_N^H reactions **3a** and **4a** or **3b** and **4b**, respectively, as the main products (Scheme 2). Formation of imino nitroxides **4a,b** demonstrates that the presence of the nitronyl nitroxide group steers the aromatization of the σ^H adducts into the eliminative route. It is important that in this case the auxiliary group is in the nucleophilic moiety.



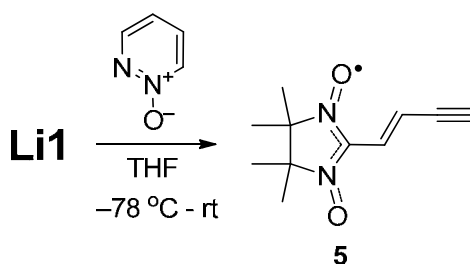
Scheme 2

The possibility of the discussed reactions involving azines was far from obvious, as the nucleophilicity of the carbanionic center in **Li1** is substantially reduced. This is the most likely reason for the failure to perform the reaction of **Li1** with mono- (quinoline) and diazines (quinoxaline, pyrimidine) to obtain the corresponding hetaryl-substituted NNs. In these cases only the initial **H1** and the known diradical **1-1** could be isolated from the reaction mixture.



When using pyridazine-*N*-oxide as the electrophilic reagent in these transformations 2-imidazoline-3-oxide-1-oxyl containing in its structure a butenynyl substituent was obtained.

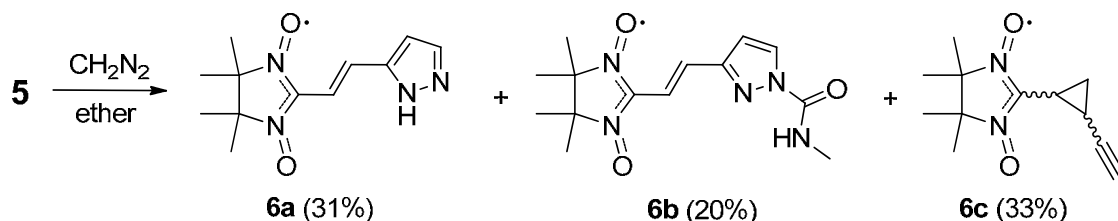
Pyridazine-*N*-oxide reacts with **Li1** in THF at -78 °C with formation, from XRD data, of exclusively *E*-isomer **5** in 68% yield. The enyne-substituted NN **5** is a “stable” at ambient conditions dark-blue crystalline solid that decomposes only upon heating to ~94–98 °C (Scheme 3). It should be noted that the works of Okusa *et al.*⁸ and Igeta *et al.*⁹ describe the opening of the pyridazine cycle in *N*-oxide under the action of Grignard reagents (ArMgBr), where the reactions also proceed mostly with formation of 1-arylbut-1-en-3-yne.

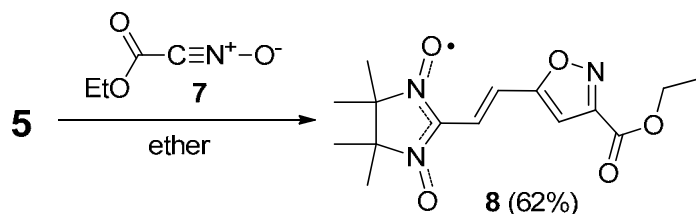


Scheme 3

With the development of an efficient method for production of **5** bearing reactive synergistic groups the latter could be used as the basic paramagnetic building block for production of new NNs. Let us first consider the reactions of 1,3-dipolar cycloaddition. It was found that **5** slowly reacts with CH₂N₂ in ether to form a mixture of two main products, pyrazolylvinyl-substituted NN **6a** and a compound with 2-ethynylcyclopropyl substituent **6c**. The regioselectivity of CH₂N₂ addition to triple bond is readily explained by taking into account the strongly π -electron-withdrawing and unsaturated character of the nitronyl nitroxide group.

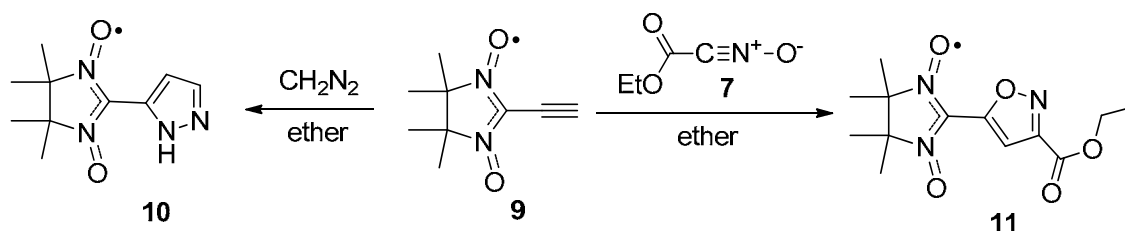
1,3-Dipolar cycloaddition of CH₂N₂ to activated double bond probably produces pyrazolines that easily lose a molecule of nitrogen to form a mixture of two geometric isomers of cyclopropane **6c**. In certain cases we also isolated amide **6b** as a minor product. Its possible origin is the reaction of **6a** with methyl isocyanate,¹⁰ which is formed in the samples of *N*-nitroso-*N*-methyl urea upon storage (Scheme 4).¹¹ Regioselectivity was also observed in the interaction of **5** with *N*-oxide of nitrile **7** generated *in situ* from ethyl chlorooximidoacetate in the presence of Et₃N¹² that produced a disubstituted isoxazole **8**.





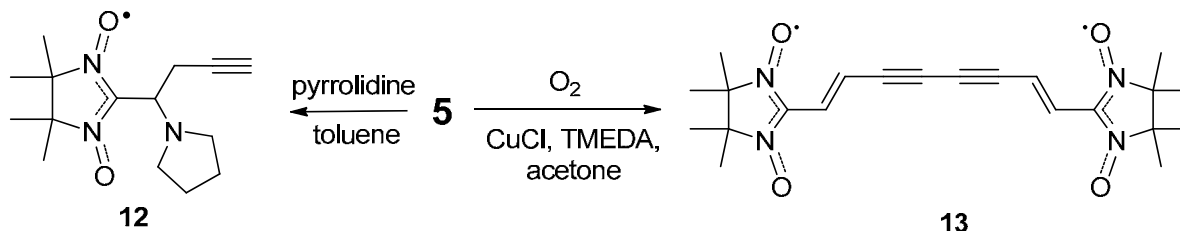
Scheme 4

Thus in the reactions of 1,3-dipolar cycloaddition enyne **5** behaves as a vinylog of ethynyl-substituted NN **9**,¹³ which upon interaction with CH₂N₂ readily forms 3(5)-pyrazolyl-substituted NN **10**, and in the reaction with **7** produces a spin-labeled isoxazole **11** (Scheme 5).



Scheme 5

At the same time nitroxides **5** and **9** behave quite differently in the reactions with secondary amines. Thus, while **9** in reaction with pyrrolidine forms exclusively the product of *trans*-addition,¹⁴ for **5** the nucleophilic attack proceeds at the α-carbon of the double bond to produce a mixture of optical isomers **12** (Scheme 6).



Scheme 6

The sensitivity of **5** to the presence of nucleophilic reagents in the reaction mixture probably precluded its oxidative coupling in classic variants (Cu(OAc)₂, Py, 60–70 °C¹⁵ and O₂, CuCl, Py¹⁶), as terminal alkyne **5** in these conditions rapidly decomposes. On the other hand, in the presence of a sterically hindered amine and CuCl¹⁷ the reaction proceeded smoothly to produce diradical **13** in 50% yield.

Crystal structures and magnetic properties

Nitroxides **3a**, **4a**, and **5** upon crystallization from a mixture of CH_2Cl_2 with *n*-heptane formed solid phase as very thin flakes adhering to each other. For compounds **3a**, **4a**, **4b**, and **5** single crystals could be selected and analyzed by XRD. The latter demonstrated that the structure of radicals **3a**, **4a**, and **4b** is characterized by a large value of the dihedral angle α between the median plane of the paramagnetic fragment and the plane of the heterocycle: the angle α is equal to 58.9° in **3a** and 69.6° in **4a**, while in two crystallographically independent radicals **4b** the value of α reaches 89.7 and 86.0° (Figure 1). The twist of the heterocycles is caused by the presence of vicinal phenyl substituent in **3a** and **4a**, with the angle between its plane and the plane of the triazine moiety being in the range 39.9 – 57.3° , and the phenyl cycle remote from the paramagnetic substituent being twisted by a smaller angle of 13.4 – 18.5° . Breaking of the conjugation between the paramagnetic moiety and the heterocycle imparts a non-typical for the family of NNs brown-reddish color to crystals of **3a** and **3b**, which is preserved after dissolution of these paramagnetics, e.g., in CH_2Cl_2 .

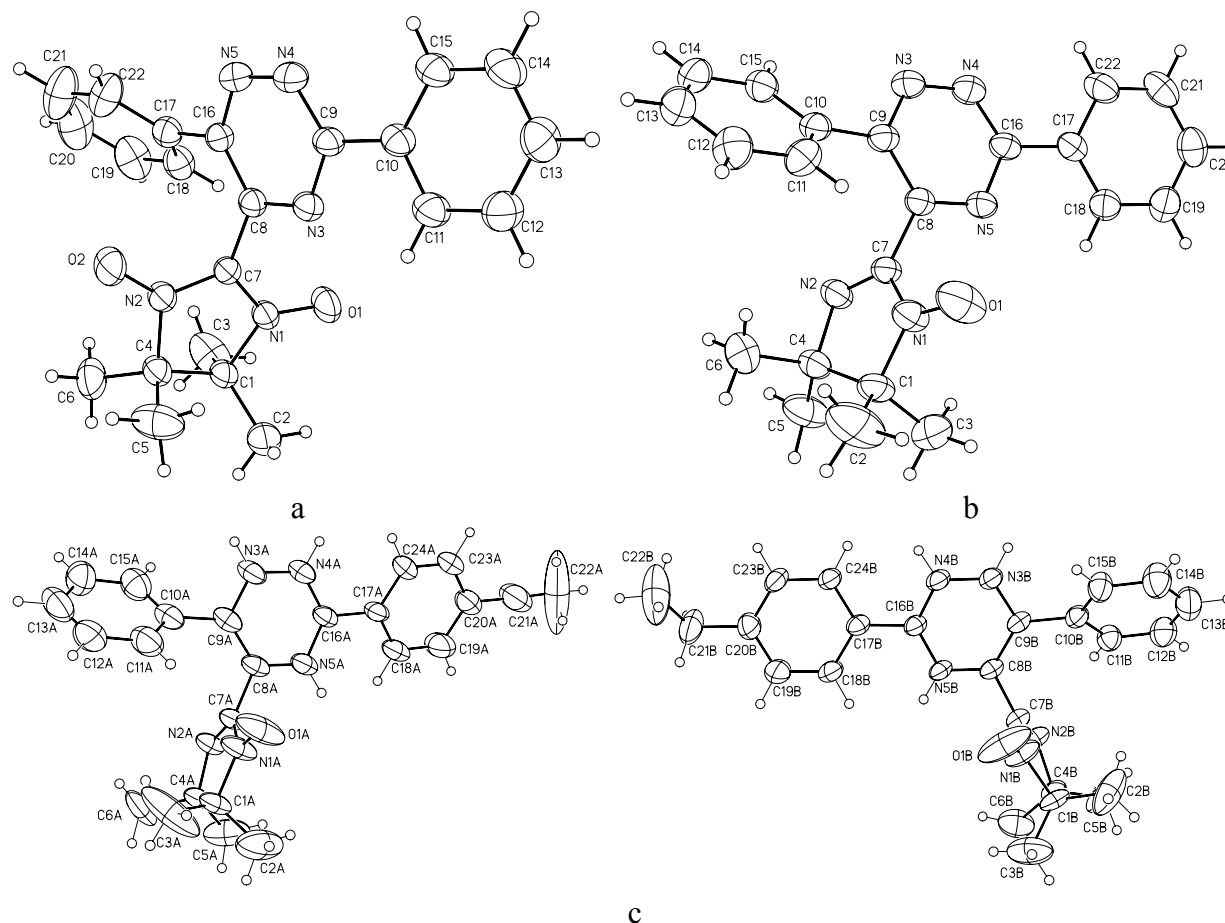


Figure 1. Structures of nitroxides **3a** (a), **4a** (b), and **4b** (c).

An important parameter for the crystal structure of nitroxides is the intermolecular distance between the paramagnetic centers, the oxygens in the N–O groups. In the structures of **3a** and **4a,b** these distances exceed 4.0 Å, which implies for them a typical behavior for a weakly coupled spin system. Indeed, the experimentally found values of effective magnetic moment (μ_{eff}) for **3a** and **4a,b** in the range 300 to 15 K are constant and close to 1.73 B.M. In the case of **3a** the value of μ_{eff} increases up to 1.88 B.M. with decreasing the temperature down to 2 K, indicating the domination of weak ferromagnetic interactions in solid state, for **4a,b** the value of μ_{eff} somewhat decreases upon cooling, pointing to a weak antiferromagnetic coupling between the unpaired electrons of the paramagnetic centers, while for **3b** it remains unchanged (see Supporting Information).

The breaking of the conjugation between the nitronyl nitroxide moiety and the π -system of the substituent mentioned above for **3a** and **4a,b** is not present in **5**, since according to XRD data the angle α (the angle between the planes of ONCNO and $-\text{CH}=\text{CH}-\text{C}\equiv\text{CH}$) for it is only 5.7°, and the distance C1–C8 of 1.435(2) Å is substantially shorter than single C–C bonds (Figure 2). For nitroxide **5** the bond lengths C8–C9, C10–C11, and C9–C10, equal to 1.317(2), 1.163(2), and

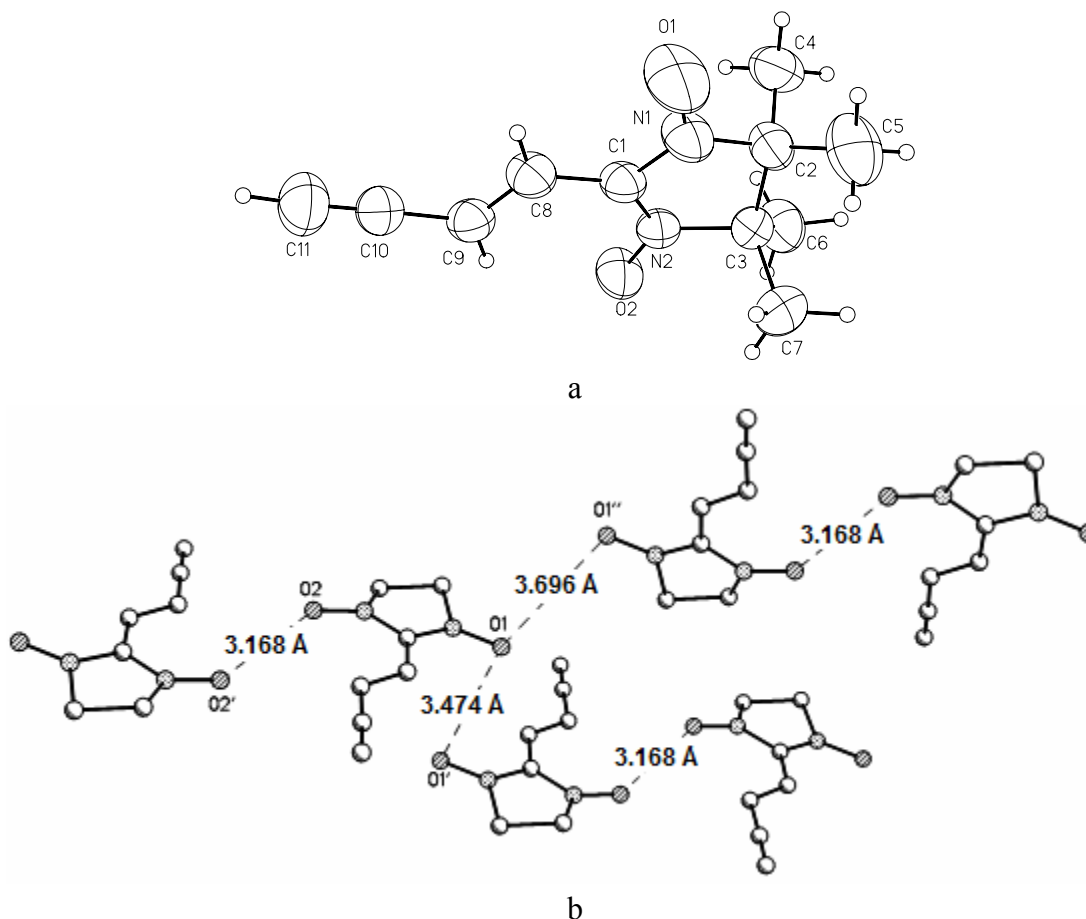


Figure 2. Structure of **5** (a) and intermolecular contacts (b) in the solid nitroxide **5**.

1.422(2) Å, respectively, correspond to data for conjugate systems $C=C-C\equiv C$.¹⁸ The distances in the N–O groups are practically equal, – N2–O2 1.278(1) and N1–O1 1.277(1) Å. Short intermolecular contacts O2...O2' (3.168 Å) are realized in solid **5** that couple the radicals into exchange-coupled dimer. In full agreement with this the experimental dependence $\mu_{\text{eff}}(T)$ is well described within the Bleaney-Bowers model¹⁹ for two-center $S = 1/2$ exchange clusters taking into account inter-dimer interactions in the molecular field approximation,²⁰ $g = 2$, $J = -39$ K, and $nJ' = -1.3$ K. (see Supporting Information).

Unequivocal determination of the structures of nitronyl nitroxides **6a** and **6b** required their XRD study. The necessary single crystal samples were obtained by slowly evaporating solutions of **6a** and **6b** in the mixture of CH_2Cl_2 with *n*-heptane. It was found that the structure of **6a** is built by a packing of dimers forming via N–H...O hydrogen bonding of the radicals between the NH group of the pyrazolyl cycle and the oxygen of one of the NO groups (O...O distance is equal to 3.778 Å) (Figure 3). This allowed to determine the position of the NH fragment in the pyrazolyl

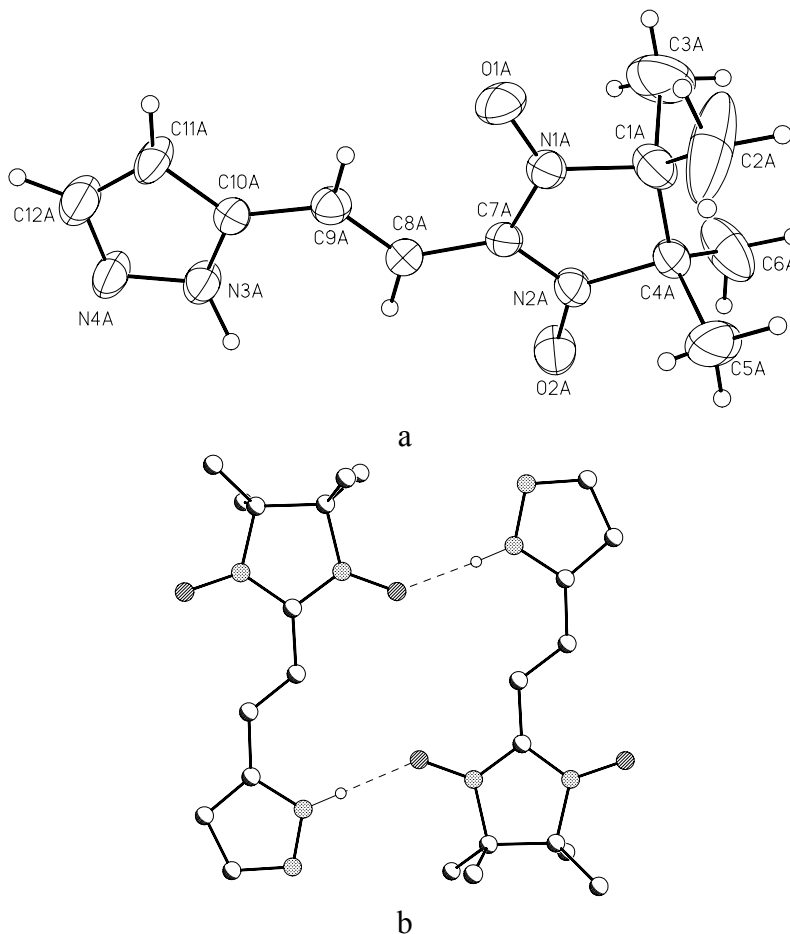


Figure 3. Structure of **6a** (a) and H-bonded dimer (b) in the solid nitroxide **6a**.

ring and thus to demonstrate the regiospecificity of the reaction of CH_2N_2 addition to triple bond of the enyne **5**. Although two crystallographically independent molecules of **6a** are present in the structure of **6a**, their geometric parameters are practically identical. The largest difference is found for the angle between the plane of the pyrazolyl ring and the ONCNO fragment: in one half of the nitroxides it is equal to 9.4° , and in another part 10.4° . The lengths of the N–O bonds fall in the range 1.270(5)–1.291(5) Å. O...O contacts (3.778 and 3.781 Å) were found between dimers that lead to chains in the structure.

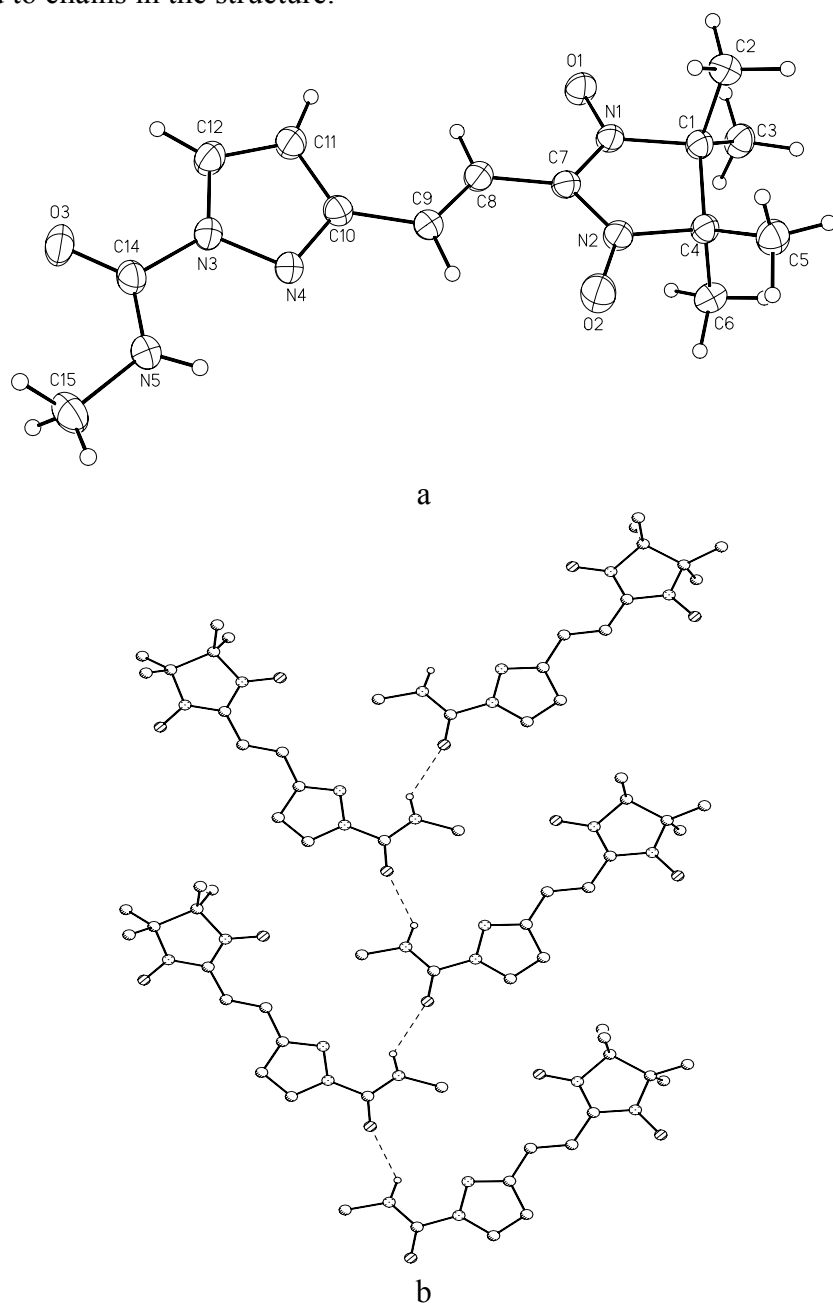


Figure 4. Structure of **6b** (a) and H-bonded chain (b) in the solid nitroxide **6b**.

In radical **6b** the value of the angle between the plane of the pyrazole cycle and the NCN fragment of the imidazoline cycle is somewhat higher than in **6a** and is equal to 15.4°. The nitroxides are linked into chains due to N–H...O type hydrogen bonds between the amide groups (Figure 4). The experimentally found value of μ_{eff} (1.73±0.01 B.M.) for **6b** at 75 K corresponds to theoretical value for a monoradical. Upon cooling of the samples below 25 K a decrease in the value of μ_{eff} is observed indicating weak exchange interactions of antiferromagnetic character between the paramagnetic centers (see Supporting Information).

After recrystallization, nitroxide **6c** was always isolated from mother solutions in the form of oil. It crystallized only as a trinuclear complex with copper(II) hexafluoroacetylacetonate [(Cu(hfac)₂)₃(**6c**)₂]·C₇H₁₆, isolated as violet crystals by slowly evaporating the mixture of *n*-heptane containing equivalent amounts of Cu(hfac)₂ and **6c** (see Supporting Information).

Crystals of diradical **13** were grown from a mixture of ethyl acetate with *n*-heptane. According to XRD data bond lengths in N–O groups are typical for nitroxides and fall in the range 1.26–1.30 Å, the lengths of the C10–C11 and C10A–C11A bonds correspond to triple bonds (1.20(2) Å), and C8–C9 and C8A–C9A (1.29(2) and 1.32(2) Å) bonds – to double bonds (Figure 5). In diradical **13**, similar to enyne **5**, single bonds C7–C8, C7A–C8A, and C11–C11A are significantly shorter than 1.54 Å typical for single bonds. The angle between the planes of the NCN fragments of the imidazoline cycles in diradical **13** is equal to 48.3°. The diradical nature of **13** is supported by its value of the effective magnetic moment (μ_{eff}), which in the range 75–300 K is practically constant and equal to 2.45 B.M. (see Supporting Information). Since the intermolecular distances between the oxygens of the nitroxide groups are rather large (more than 4.46 Å), the μ_{eff} (*T*) dependence displayed by **13** is determined by intramolecular antiferromagnetic exchange between the unpaired electrons. Indeed the experimental dependence μ_{eff} (*T*) is well described within the Bleaney-Bowers model¹⁹ for isolated two-center *S* = 1/2 exchange clusters with *g* = 2.0 and *J* = –16 K.

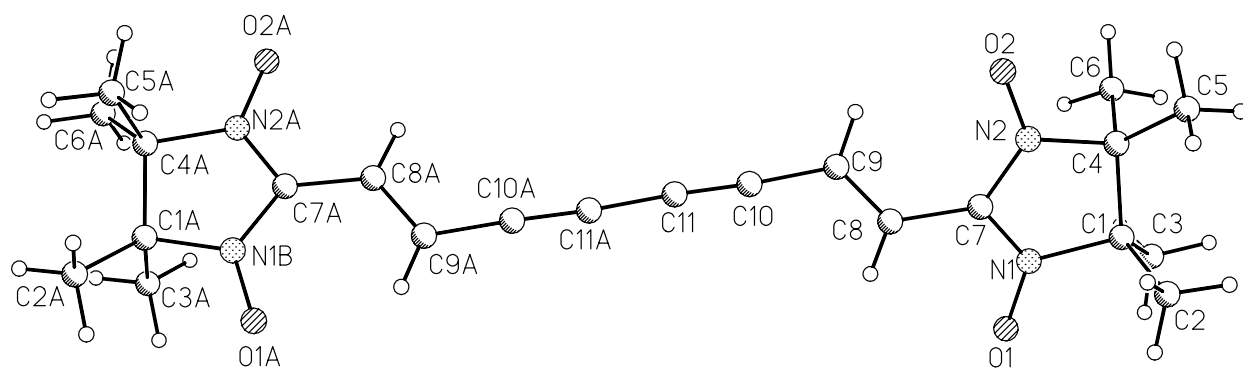


Figure 5. Structure of diradical **13**.

Electron paramagnetic resonance

Figure 6a shows the experimental and simulated ESR spectra for **5**. The experimental spectrum was taken in a degassed toluene solution at room temperature, concentration about 10^{–5} M, the

estimated accuracy of determination of the hyperfine constants is 0.005 mT (half of the modulation amplitude of 0.01 mT), g-value was measured using solid DPPH as the reference. Modeling of spectra yielded: $A_{N1} = 0.749$ mT, $A_{N2} = 0.726$ mT, $A_{12H} = 0.021$ mT, $A_{H1} = 0.146$ mT, $A_{H2} = 0.120$ mT, $A_{H3} = 0.067$ mT, $g_{iso} = 2.0065$. The values of the nitrogen hyperfine couplings show that the two nuclei are not completely equivalent in solution due to a relatively rigid extended π -system encompassing the imidazoline moiety and the substituent. Furthermore, ESR spectra show rather pronounced alternating linewidth effect due to modulation of nitrogen couplings,²¹ most probably because of “wiggling” the substituent with respect to the imidazoline ring.

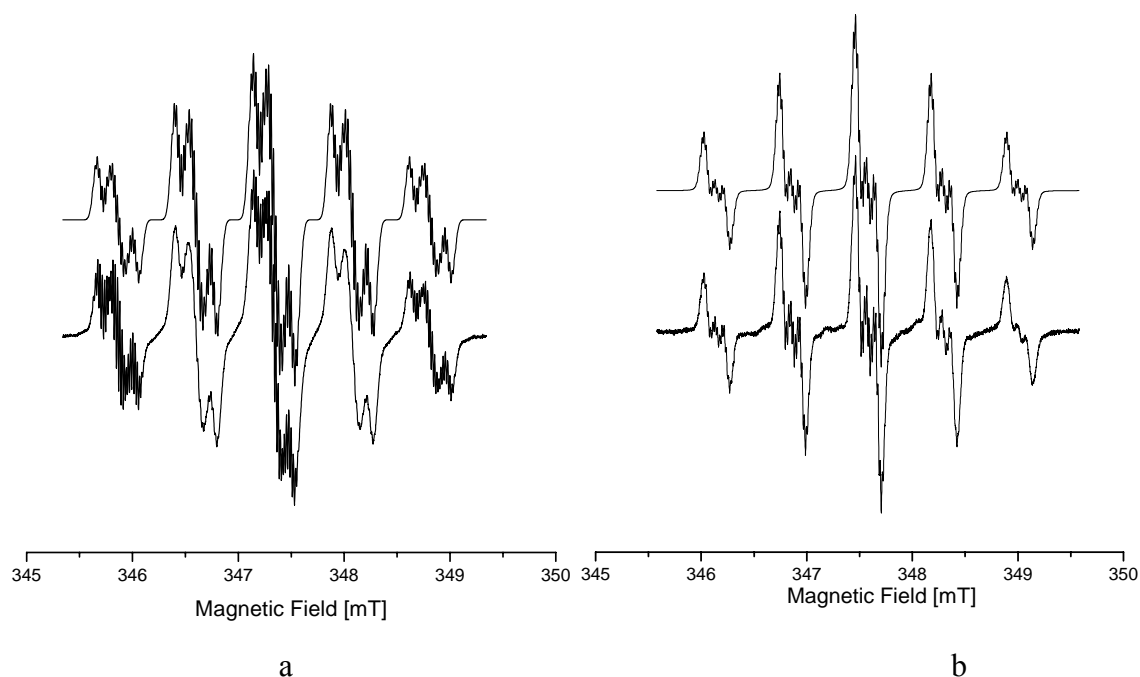


Figure 6. ESR spectra of **5** (a) and **3a** (b): experimental (bottom trace) and the result of their modeling (top trace).

Experimental and simulated ESR spectra for **3a** are shown in Figure 6b. Modeling yielded: $A_{2N} = 0.717$ mT, $A_{12H} = 0.017$ mT, $A_{Na} = 0.086$ mT, $A_{Nb} = 0.022$ mT, $A_{Nc} = 0.012$ mT, $g_{iso} = 2.0065$. The dominant structure of the spectrum comes from two equivalent imidazoline nitrogens, one nitrogen from the substituent, and 12 protons from the four guarding methyl groups. Two other nitrogens have rather small hyperfine coupling constants, which are not reliably determined from simulations. The spectrum for **3b** (not shown) is almost identical, as the two radicals differ only in a remote ethyl group in the substituent that has practically no effect on the spectrum. Modeling yielded: $A_{2N} = 0.716$ mT, $A_{12H} = 0.018$ mT, $A_{Na} = 0.086$ mT, $A_{Nb} = 0.019$ mT, $A_{Nc} = 0.011$ mT, $g_{iso} = 2.0065$.

Figure 7a shows ESR spectrum for **4a** (bottom trace) and its modeling (top trace) that yielded the following parameters: $A_{N1} = 0.855$ mT, $A_{N2} = 0.431$ mT, $A_{12H} = 0.019$ mT, $A_{Na} = 0.054$

mT, $A_{Nb}=0.012$ mT, $A_{Nc}=0.007$ mT, $g_{iso}=2.0059$. The characteristically looking spectrum is dominated by two imidazoline nitrogens with the ratio of hfc's approximately 1:2, with an additional nitrogen from substituent and 12 protons from the guarding methyls. Two further nitrogens with minor couplings were introduced into simulations, but these constants are too small to be reliable. As with **3a/b**, the spectrum for **4b** is very similar, as it is not sensitive to the remote ethyl. The extracted parameters are as follows: $A_{N1}=0.856$ mT, $A_{N2}=0.431$ mT, $A_{12H}=0.019$ mT, $A_{Na}=0.054$ mT, $A_{Nb}=0.012$ mT, $A_{Nc}=0.008$ mT, $g_{iso}=2.0060$, with two smaller couplings being not very reliable.

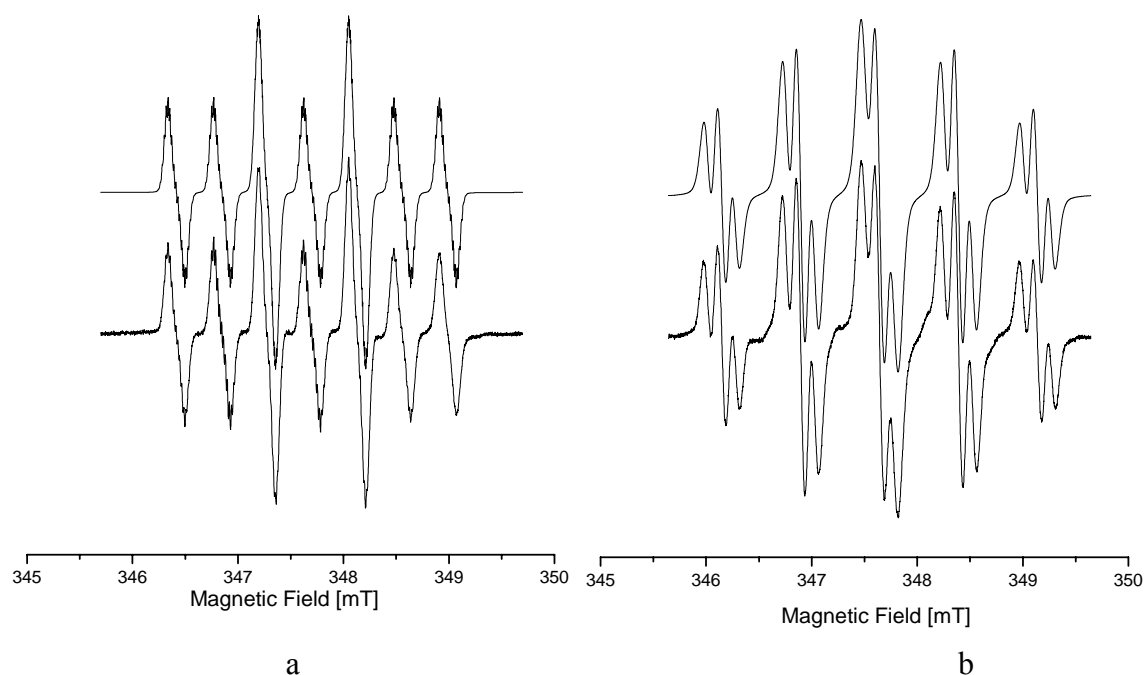


Figure 7. ESR spectra of **4a** (a) and **6a** (b): experimental (bottom trace) and the result of their modeling (top trace).

Figure 7b shows the spectra for **6a**. The dominant structure comes from two slightly non-equivalent imidazoline nitrogens, due to locked structure of the radical in solution with hindered relative motion of the imidazoline and the substituent, and two bridge protons. The spectrum is not resolved, but the standard substructure of 12 protons from the four guarding methyl groups reproduces the widths of the lines. Further nuclei with small hfc's could have been introduced in modeling, but the spectrum does not warrant this as it lacks finer details that need to be reproduced in simulations. The parameters are: $A_{N1}=0.732$ mT, $A_{N2}=0.762$ mT, $A_{12H}=0.016$ mT, $A_{Ha}=0.137$ mT, $A_{Hb}=0.114$ mT, $g_{iso}=2.0066$.

Figure 8a shows ESR spectra for **8**. Modeling (the top spectrum) yielded: $A_{N1}=0.735$ mT, $A_{N2}=0.725$ mT, $A_{12H}=0.019$ mT, $A_{Ha}=0.122$ mT, $A_{Hb}=0.139$ mT, $A_{Hc}=0.026$ mT, $A_{Na}=0.036$ mT, $g_{iso}=2.0066$. The dominant structure comes from two nearly equivalent imidazoline nitrogens

(this produces the alternating resolved/unresolved substructures of the lines in the quintet), two bridge protons, and 12 methyl protons.

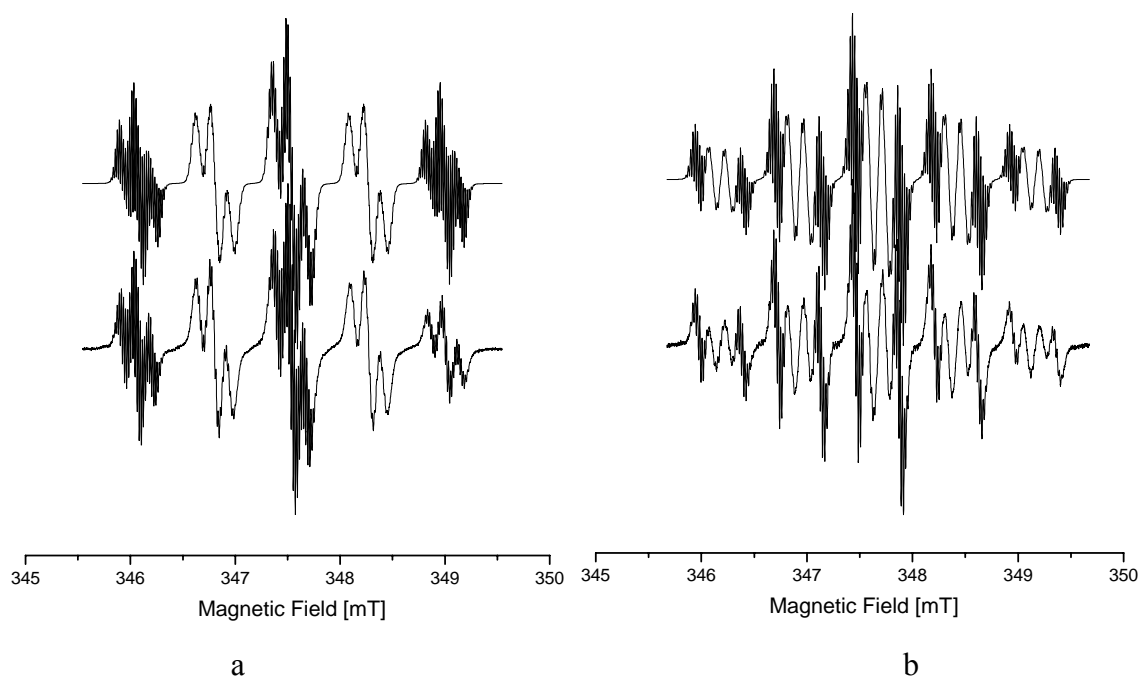


Figure 8. ESR spectra of **8** (a) and **12** (b): experimental (bottom trace) and the result of their modeling (top trace).

Figure 8b shows the rather weird looking spectrum for **12** that was well reproduced in modeling (top trace). The spectrum has a peculiar substructure of the lines of the 12321 quintet from two imidazoline nitrogens – a quartet of lines with two outermost lines showing a resolved substructure, while the two inner lines are unresolved. The dominant structure comes from two equivalent imidazoline nitrogen (the modeling invariably produced equal values for two independently varied couplings), one proton and one nitrogen with rather large couplings, a standard set of 12 methyl protons, and two slightly different protons, most likely methylene ones (it is their “difference” that produces the specific look of the spectrum). The obtained parameters are: $A_{2N}=0.744$ mT, $A_{12H}=0.022$ mT, $A_{Ha}=0.115$ mT, $A_{Na}=0.146$ mT, $A_{Hb}=0.037$ mT, $A_{Hc}=0.026$ mT, $g_{iso}=2.0066$.

Spectra for **6c** in Figure 9a show the dominating structure from two equivalent imidazoline nitrogens and 12 methyl protons, but reproduction of the width of the lines (having a resolved substructure) required introduction of further nuclei with small hfc's consistent with the chemical structure of the radical (three independent protons and two equivalent protons in the cyclopropane ring). The modeling reproducibly gives equivalent coupling for the two imidazoline nitrogens, and yielded the following parameters: $A_{2N}=0.747$ mT, $A_{12H}=0.021$ mT, $A_{Ha}=0.044$ mT, $A_{Hb}=0.028$ mT, $A_{Hc}=0.023$ mT, $A_{2H}=0.046$ mT, $g_{iso}=2.0064$.

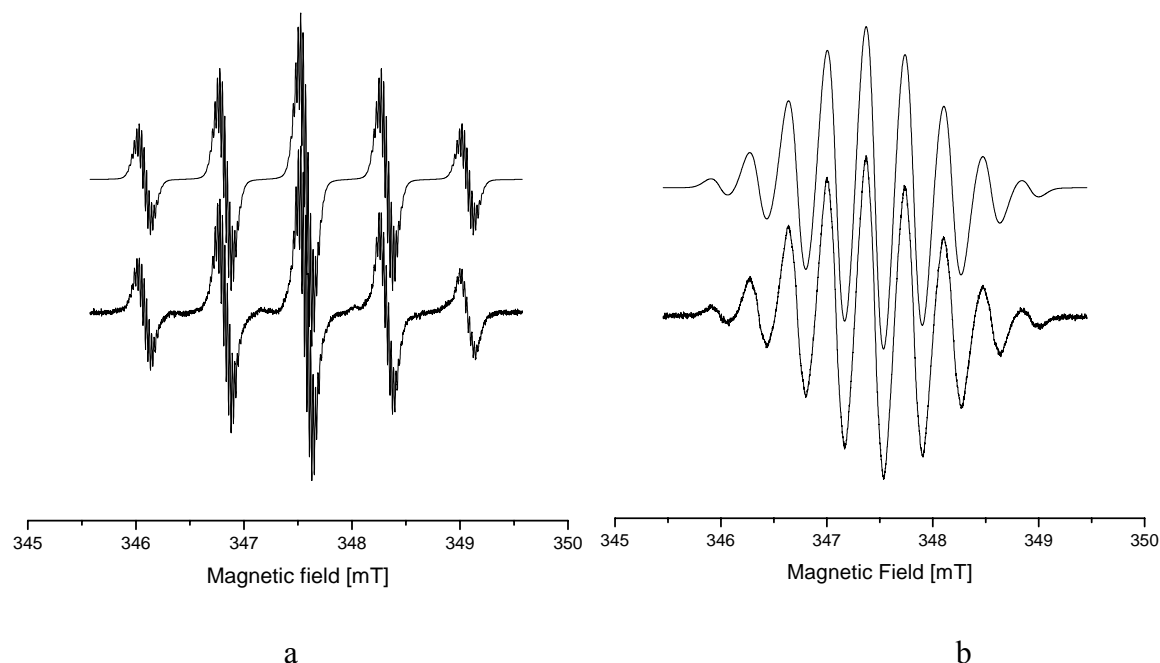


Figure 9. ESR spectra of **6c** (a) and **13** (b): experimental (bottom trace) and the result of their modeling (top trace).

Finally, the Figure 9b shows the spectra for diradical **13** and its modeling that faithfully reproduces the experiment. The spectrum corresponds to fast exchange limit with couplings to four equivalent nitrogens of two imidazoline moieties $A_{4N}=0.365$ mT and the peak-to-peak width of unresolved lines $\Delta H_{pp}=0.091$ mT, $g_{iso}=2.0064$. The diradical is rather stable in degassed toluene solution, and after about ten hours, when the temperature of solution was varied from 183K to 353K (approximately melting and boiling points of toluene) and the sample was then cooled down back to room temperature, gave the same spectrum as the freshly prepared sample, both in terms of shape and intensity. No signs of monoradical spectra were traced, and there were no changes to the spectrum itself during the extended temperature experiment apart from the expected transformation from non-isotropic to isotropic spectrum upon melting of the matrix, and additional line broadening due to accelerated spin exchange at elevated temperatures. The diradical is thus kinetically and magnetically stable in degassed toluene solution.

Conclusions

In this work convergent schemes of nitroxide synthesis based on S_N^H reactions of 4,4,5,5-tetramethyl-4,5-dihydro-1H-imidazol-3-oxide-1-oxyl lithium salt with activated azines, 3,6-diaryl-1,2,4-triazines and pyridazine-*N*-oxide are suggested. Using these schemes a broad range of new polyfunctional nitronyl and imino nitroxides was obtained, viz.: 1,2,4-triazinyl-, buten-3-ynyl-, 2-(1H-pyrazol-5-yl)vinyl-, 2-ethynylcyclopropyl-, 2-(3-(ethoxycarbonyl)isoxazol-5-

yl)vinyl-, 1-(pyrrolidin-1-yl)but-3-ynyl-substituted nitronyl nitroxides, as well as a diradical, 2,2'-((1*E*,7*E*)-octa-1,7-dien-3,5-diyne-1,8-diyl)bis(4,4,5,5-tetramethyl-4,5-dihydro-1*H*-imidazol-3-oxide-1-oxyl). The results of this work expand the views of the synthetic potential of S_N^H reactions and may prove useful for the development of synthetic strategies towards new magnetoactive systems.

Experimental Section

General. Pyridazine-1-oxide,²² 2,3-bis(hydroxyamino)-2,3-dimethylbutane sulphate monohydrate²³ and ethyl 2-chloro-2-(hydroxyimino)acetate²⁴ **8** were synthesized as described in literature. THF was distilled from sodium benzophenone ketyl in a recycling still. Other reagents and solvents from commercial sources were of the highest purity available and were used as received. The reactions were monitored by TLC using “Silica gel 60 F₂₅₄ aluminum sheets, Merck”. Chromatography was carried out with the use of “Merck” silica gel (0.063–0.100 mm for column chromatography) for column chromatography. C, H, and N elemental analyses were carried out by the Chemical Analytical Center of the Novosibirsk Institute of Organic Chemistry. The melting points were determined on a Boethius apparatus and were not corrected. Infrared spectra (4000–400 cm⁻¹) were recorded with a Bruker VECTOR 22 instrument in KBr pellets. UV/Vis spectrum of diradical **13** was registered with Hewlett Packard 8453 spectrophotometer. X-Band CW ESR spectra were recorded in dilute degassed toluene solutions at room temperature on a Bruker EMX spectrometer and modeled in free package Winsim v.0.96 as described earlier.²⁵ The magnetochemical experiment was run on an MPMS-5S (“Quantum Design”) SQUID magnetometer at temperatures from 2 K to 300 K in a homogeneous external magnetic field of up to 49.5 kOe. The molar magnetic susceptibility χ was calculated using Pascal’s additive scheme including diamagnetic corrections.

4,4,5,5-Tetramethyl-4,5-dihydro-1*H*-imidazol-3-oxide-1-oxyl (H1).³ **Stage 1.** To the suspension of 2,3-bis(hydroxyamino)-2,3-dimethylbutane sulphate monohydrate (25 g, 0.095 mol) in 80 ml of water 37% aqueous solution of CH₂O (8.1 g, 0.1 mol) was added dropwise over the period of 30 minutes (the reaction is conveniently performed in a high 200 ml flask). The solution was quenched with NaHCO₃ (using 1–5 ml of benzene to inhibit foaming) until no more CO₂ was evolving. The white product was filtered off, washed with water, washed with acetone, air-dried, and recrystallized from MeOH with filtration (about 250 ml of MeOH was needed to recrystallize 2 g). Yield of 4,4,5,5-tetramethylimidazoline-1,3-diol is 6.95 g (46%), mp. 153–165 °C (accompanied by evolution of gas bubbles). IR: ν = 494, 515, 548, 594, 753, 795, 908, 954, 1016, 1060, 1093, 1120, 1145, 1163, 1279, 1331, 1368, 1389, 1454, 2883, 2986, 3220 broad cm⁻¹. ¹H NMR (400 MHz, DMSO-*d*₆): δ 0.96 (s, 12 H, Me); 3.87 (s, 2 H, CH₂); 7.64 (s, 2 H, OH). ¹³C NMR (100 MHz, DMSO-*d*₆): δ 79.8 (C²), 67.1 (C^{4,5}), 20.2 broad (CH₃).

Stage 2. To a cooled at about 5 °C mixture of 4,4,5,5-tetramethylimidazoline-1,3-diol (16 g, 0.1 mol), CHCl₃ (150 ml) and water (150 ml) NaIO₄ (34.2 g, 0.16 mol) was added in small portions under stirring over the period of 40 min. After further stirring for 30 min the organic layer was separated. The aqueous layer was filtered (from NaIO₃) and extracted with CHCl₃ (3×30 ml). The organic phases were combined, dried over Na₂SO₄ and filtered through a layer of Al₂O₃ (2×15 cm). The solution was diluted with 30 ml of *n*-heptane and evaporated (pressure 70 mm Hg, bath at room temperature) until the onset of product crystallization, after which the flask was kept at about –10 °C for 20 h. The residue was filtered off and washed on filter with cold *n*-hexane to give 13.8 g (88%) of 0.5–3 mm dark-red crystals covered with small yellowish crystals visible in a microscope. The product, which according to TLC and IR data contained a minute amount of 1,3-dihydroxy-4,4,5,5-tetramethylimidazolidyn-2-one and 2-iodo-4,4,5,5-tetramethyl-4,5-dihydro-1*H*-imidazol-3-oxide-1-oxyl, was used in synthesis without additional purification, because in the course of the differentiating procedures the content of admixtures further increased. To prepare a reference sample nitroxide **H1** was crystallized from *n*-hexane, and dark-red flakes were manually selected from the deposited crystals, mp. 125–127 °C. IR: ν = 3075, 2988, 1454, 1403, 1372, 1323, 1268, 1199, 1136, 956, 819, 775, 692, 613, 564, 531, 431 cm^{–1}.

3,6-Diphenyl-1,2,4-triazine (2a) was prepared from 3,6-diphenyl-1,2,4-triazine-4-oxide according to literature,²⁶ yield 75%, yellow needles, mp 157–160 °C with decomposition (lit.²⁷ 160 °C).

3-(4-Ethylphenyl)-6-phenyl-1,2,4-triazine (2b) was prepared from 3-(4-ethylphenyl)-6-diphenyl-1,2,4-triazine-4-oxide; yield 85%, yellow powder, mp. 140 °C, *R*_f 0.30 (C₆H₆). IR: ν = 581, 686, 764, 801, 849, 1017, 1029, 1085, 1178, 1312, 1399, 1416, 1442, 1505, 1556, 1582, 1606, 2864, 2925, 2959, 3030, 3054 cm^{–1}. ¹H NMR (400 MHz, DMSO-*d*₆/CCl₄): δ 1.31 (t, 3 H, *J* = 7.52 Hz, CH₃); 2.75 (q, 2 H, *J* = 7.52 Hz, CH₂); 7.38 (m, 2 H, Ph); 7.39–7.60 (m, 3 H, Ph); 8.23 (m, 2 H, C₆H₄); 8.42 (m, 2 H, C₆H₄); 9.33 (s, 1 H). Anal. Calcd. for C₁₇H₁₅N₃ (262.33): C, 78.13; H, 5.79; N, 16.08. Found: C, 78.26; H, 5.67; N, 16.23.

(E)-2-(But-1-en-3-ynyl)-1-hydroxy-4,4,5,5-tetramethyl-4,5-dihydro-1*H*-imidazol-3-oxide-1-oxyl (5). To a vigorously stirred solution of **H1** (157 mg, 1.0 mmol) in 3 ml of absolute THF a 2.0 M solution of LDA (or 1.06 M of LiN(SiMe₃)₂) in THF (1.1 mmol) was added at –78 °C under argon atmosphere. The reaction mixture was stirred at –78 °C for 20 min. To the obtained bright-red solution of the lithiated derivative **Li1** a solution of pyridazine-*N*-oxide (106 mg, 1.1 mmol) in 4 ml of THF was added at –78 °C under argon atmosphere, and the reaction mixture turned into a greenish-brown suspension. The cooling bath was removed; the reaction mixture was stirred for 2 h and concentrated in vacuo. The obtained residue was put through a column with SiO₂ using ethylacetate as the eluent. The blue-colored fraction was evaporated until dry under reduced pressure, the obtained residue was recrystallized from a mixture of *n*-heptane and CH₂Cl₂. Yield 141 mg (68%), blue-green crystals, mp. 94–98 °C (with decomposition), *R*_f 0.65 (EtOAc). IR: ν = 3259, 3067, 3042, 2993, 2925, 2853, 2613, 2094, 1824, 1593, 1479, 1449, 1425, 1386, 1370, 1284, 1263, 1217, 1165, 1136, 1022, 979, 861, 679, 637, 616, 541, 483, 475,

424 cm^{-1} . $\mu_{\text{eff}} \sim 1.73 \mu_{\text{B}}$ (200–300 K). Anal. Calcd. for $\text{C}_{11}\text{H}_{15}\text{N}_2\text{O}_2$ (207.25): C, 63.75; H, 7.30; N, 13.52. Found: C, 63.80; H, 7.55; N, 13.14.

4,4,5,5-Tetramethyl-2-(3,6-diphenyl-1,2,4-triazin-5-yl)-4,5-dihydro-1H-imidazol-3-oxide-1-oxyl (3a) and 4,4,5,5-tetramethyl-2-(3,6-diphenyl-1,2,4-triazin-5-yl)-4,5-dihydro-1H-imidazol-1-oxyl (4a). To a stirred solution of **H1** (157 mg, 1.0 mmol) in 3 ml THF a 2.0 M solution of LDA (or 1.06 M of $\text{LiN}(\text{SiMe}_3)_2$) in THF (1.1 mmol) was added at -78°C under argon atmosphere. The reaction mixture was stirred at -78°C for 20 min. To the obtained bright-red solution of **Li1** a solution of 3,6-diphenyl-1,2,4-triazine **2a** (256 mg, 1.1 mmol) in 6 ml THF was added at -78°C under argon atmosphere. The obtained burgundy-colored suspension was stirred for 2 h at room temperature and concentrated in vacuo. The residue was purified on a column with SiO_2 using a mixture of benzene and ethyl acetate (9:1) as the eluent. The fractions containing **3a** and **4a** were concentrated at reduced pressure, the residues were recrystallized from a mixture of *n*-heptane with CH_2Cl_2 , the produced crystals were dried in vacuum.

Compound (3a). Yield 123 mg (32%), brown-red crystals, mp $180\text{--}181^\circ\text{C}$, R_f 0.15 (C_6H_6 – ethyl acetate, 9:1). IR: $\nu = 3061, 2991, 2976, 2926, 2868, 1601, 1524, 1500, 1453, 1417, 1395, 1369, 1261, 1219, 1182, 1136, 1072, 1055, 1024, 918, 873, 775, 699, 556, 473 \text{ cm}^{-1}$. HRMS, m/z : 388.1774 (M^+ , calcd. for $\text{C}_{22}\text{H}_{22}\text{N}_5\text{O}_2$ 388.1768). MS, m/z (%): 388 (M^+ , 100), 288 (11), 259 (13), 257 (41), 169 (10), 129 (10), 128 (13), 127 (27), 105 (34), 103 (15), 84 (43), 69 (27). $\mu_{\text{eff}} \sim 1.73 \mu_{\text{B}}$ (50–300 K). Anal. Calcd. for $\text{C}_{22}\text{H}_{22}\text{N}_5\text{O}_2$ (388.45): C, 68.0; H, 5.7; N, 18.0. Found: C, 68.1; H, 5.9; N, 18.0.

Compound (4a). Yield 130 mg (35%), bright-orange crystals, mp $163\text{--}165^\circ\text{C}$, R_f 0.40 (C_6H_6 – ethyl acetate, 9:1). IR: $\nu = 3061, 2991, 2976, 2926, 1500, 1453, 1395, 1369, 1261, 1159, 1072, 1024, 803, 769, 699, 556 \text{ cm}^{-1}$. HRMS, m/z : 373.1898 ($[\text{M}+\text{H}]^+$, calcd. for $\text{C}_{22}\text{H}_{23}\text{N}_5\text{O}$ 373.1897). MS, m/z (%): 373 ($[\text{M}+\text{H}]^+$, 3), 357 (13), 288 (13), 259 (15), 128 (12), 127 (21), 114 (15), 84 (100), 69 (28). $\mu_{\text{eff}} \sim 1.73 \mu_{\text{B}}$ (50–300 K). Anal. Calcd. for $\text{C}_{22}\text{H}_{23}\text{N}_5\text{O}$ (372.45): C, 71.0; H, 6.0; N, 18.8. Found: C, 71.0; H, 5.9; N, 18.7.

4,4,5,5-Tetramethyl-2-(3-(4-ethylphenyl)-6-phenyl-1,2,4-triazin-5-yl)-4,5-dihydro-1H-imidazol-3-oxide 1-oxyl (3b) and 4,4,5,5-tetramethyl-2-(3-(4-ethylphenyl)-6-diphenyl-1,2,4-triazin-5-yl)-4,5-dihydro-1H-imidazol-1-oxyl (4b) were obtained by the procedure described for **3a** and **4a**.

Compound (3b). Yield 124 mg (30%), brown-red crystals, mp $187\text{--}188^\circ\text{C}$, R_f 0.15 (C_6H_6 – ethyl acetate, 9:1). IR: $\nu = 2966, 2933, 1609, 1579, 1498, 1448, 1419, 1394, 1371, 1215, 1173, 1136, 1117, 1079, 1053, 1016, 972, 874, 854, 812, 766, 748, 702, 673, 626, 541, 508, 476 \text{ cm}^{-1}$. HRMS, m/z : 416.2084 (M^+ , calcd. for $\text{C}_{24}\text{H}_{26}\text{N}_5\text{O}_2$ 416.2081). MS, m/z (%): 416 (M^+ , 31), 385 (23), 384 (14), 316 (14), 287 (30), 257 (13), 169 (17), 133 (23), 131 (16), 128 (26), 127 (27), 116 (24), 105 (11), 69 (51), 41 (18), 18 (21). $\mu_{\text{eff}} \sim 1.73 \mu_{\text{B}}$ (50–300 K). Anal. Calcd. for $\text{C}_{24}\text{H}_{26}\text{N}_5\text{O}_2$ (416.50): C, 69.2; H, 6.3; N, 16.8. Found: C, 69.2; H, 6.8; N, 16.9.

Compound (4b). Yield 128 mg (32%), bright-orange crystals, mp $144\text{--}145^\circ\text{C}$, R_f 0.45 (C_6H_6 – ethyl acetate, 9:1). IR: $\nu = 2976, 2933, 1610, 1522, 1498, 1444, 1396, 1280, 1232, 1183, 1160, 1141, 1058, 1017, 865, 823, 801, 767, 700, 618, 560 \text{ cm}^{-1}$. HRMS, m/z : 401.2214 ($[\text{M}+\text{H}]^+$,

calcd. for $C_{24}H_{27}N_5O$ 401.2210). MS, m/z (%): 401 ($[M+H]^+$, 10), 385 (16), 384 (13), 316 (14), 288 (10), 287 (27), 286 (13), 169 (11), 131 (12), 128 (16), 127 (15), 116 (11), 114 (10), 84 (100), 69 (28), 41 (11), 28 (16). $\mu_{\text{eff}} \sim 1.73 \mu_B$ (50–300 K). Anal. Calcd. for $C_{24}H_{26}N_5O$ (400.50): C, 72.0; H, 6.5; N, 17.5. Found: C, 71.8; H, 6.5; N, 17.6.

(E)-2-(2-(1H-Pyrazol-5-yl)vinyl)-4,4,5,5-tetramethyl-4,5-dihydro-1H-imidazol-3-oxide 1-oxyl (6a), (E)-2-(2-(1-(methylcarbamoyl)-1H-pyrazol-3-yl)vinyl)-4,4,5,5-tetramethyl-4,5-dihydro-1H-imidazol-3-oxide 1-oxyl (6b), 2-(2-ethynylcyclopropyl)-4,4,5,5-tetramethyl-4,5-dihydro-1H-imidazol-3-oxide 1-oxyl (6c). To a stirred at 0 °C solution of enyne **2** (207 mg, 1.0 mmol) in Et_2O (30 ml) was added a solution of CH_2N_2 in Et_2O prepared following a standard method from 227 mg (2.2 mmol) of *N*-methyl-*N*-nitroso urea. The cooling bath was removed; the reaction mixture was stirred for 24 h and concentrated in vacuo. The residue was purified on a column with SiO_2 to give **6c** (*n*-hexane – $EtOAc$ 6:4), **6b** (*n*-hexane – $EtOAc$ 4:6) and **6a** (*n*-hexane – $EtOAc$ 2:8). The fractions containing **6a**, **6b**, and **6c** were concentrated at reduced pressure, the residues were crystallized from a mixture of *n*-heptane with CH_2Cl_2 .

Compound (6a). Yield 77 mg (31%), green crystals, mp. 179–181 °C, R_f 0.15 (*n*-hexane – ethyl acetate 2:8). IR: $\nu = 3211, 3106, 3032, 2988, 1627, 1562, 1451, 1399, 1374, 1321, 1256, 1211, 1166, 1136, 1105, 1050, 1027, 985, 921, 894, 873, 803, 758, 610, 542, 451, 419 \text{ cm}^{-1}$. HRMS, m/z : 249.1352 (M^+ , calcd. for $C_{12}H_{17}N_4O_2$ 249.1346). MS, m/z (%): 249 (M^+ , 73), 121 (10), 120 (12), 114 (9), 84 (100), 69 (70), 56 (16), 55 (15), 41 (28), 39 (7), 18 (13). Anal. Calcd. for $C_{12}H_{17}N_4O_2$ (249.29): C, 57.8; H, 6.9; N, 22.5. Found: C, 57.8; H, 6.6; N, 22.5.

Compound (6b). Yield 61 mg (20%), blue-green crystals, mp. 181–183 °C, R_f 0.20 (*n*-hexane – $EtOAc$ 4:6). IR: $\nu = 3368, 3107, 3030, 2987, 2945, 1709, 1625, 1520, 1454, 1419, 1371, 1361, 1274, 1253, 1238, 1213, 1163, 1138, 1058, 1030, 977, 962, 873, 809, 767, 754, 660, 538, 450, 422 \text{ cm}^{-1}$. $\mu_{\text{eff}} \sim 1.73 \mu_B$ (50–100 K). $C_{14}H_{20}N_5O_3$ (306.34): calcd. C, 54.9; H, 6.6; N, 22.9; found C, 54.8; H, 7.0; N, 22.7. IR: $\nu = 3368, 3107, 3030, 2987, 2945, 1709, 1625, 1520, 1454, 1419, 1371, 1361, 1274, 1253, 1238, 1213, 1163, 1138, 1058, 1030, 977, 962, 873, 809, 767, 754, 660, 538, 450, 422 \text{ cm}^{-1}$. $\mu_{\text{eff}} \sim 1.73 \mu_B$ (50–100 K). Anal. Calcd. for $C_{14}H_{20}N_5O_3$ (306.34): C, 54.9; H, 6.6; N, 22.9. Found: C, 54.8; H, 7.0; N, 22.7.

Compound (6c). Yield 73 mg (33%), violet oil, R_f 0.25 (*n*-hexane – ethyl acetate 6:4). IR: $\nu = 3237, 3092, 2983, 2928, 1536, 1454, 1399, 1371, 1348, 1283, 1216, 1178, 1138, 1116, 1071, 1027, 920, 867, 821, 709, 680, 618, 540, 477 \text{ cm}^{-1}$. HRMS, m/z : 221.1285 (M^+ , calcd. for $C_{12}H_{17}N_2O_2$ 221.1290). MS, m/z (%): 221 (M^+ , 19), 114 (15), 85 (7), 84 (100), 83 (13), 69 (67), 56 (12), 55 (18), 41 (32), 39 (10). Anal. Calcd. for $C_{12}H_{17}N_2O_2$ (221.28): C, 65.1; H, 7.7; N, 12.7. Found: C, 65.1; H, 7.7; N, 12.7.

(E)-2-(2-(3-(Ethoxycarbonyl)isoxazol-5-yl)vinyl)-4,4,5,5-tetramethyl-4,5-dihydro-1H-imidazol-3-oxide 1-oxyl (8). To a stirred solution of enyne **5** (207 mg, 1.0 mmol) and ethyl 2-chloro-2-(hydroxyimino)acetate (227 mg, 1.5 mmol) in dry Et_2O (35 ml) a solution of NEt_3 (0.208 ml, 1.5 mmol) in Et_2O (30 ml) was added dropwise over the period of 1 hr at 0 °C under argon atmosphere. The cooling bath was removed; the reaction mixture was stirred for 2 h and concentrated in vacuo. The obtained residue was put through a column with SiO_2 using a mixture

of hexane with ethyl acetate (7:3) as the eluent. The blue-green colored fraction was evaporated until dry under reduced pressure, the obtained residue was recrystallized from a mixture of *n*-heptane and CH₂Cl₂. Yield 200 mg (62%), green crystals, mp. 107–108 °C, *R*_f 0.15 (hexane – ethyl acetate 7:3). IR: ν = 3142, 3103, 2986, 2941, 1746, 1727, 1571, 1452, 1416, 1375, 1275, 1212, 1140, 1109, 1023, 980, 969, 834, 779, 542 cm⁻¹. HRMS, *m/z*: 322.1401 (M⁺, calcd. for C₁₅H₂₀N₃O₅ 322.1397). MS, *m/z* (%): 322 (M⁺, 31), 161 (7), 149 (10), 135 (8), 114 (9), 85 (8), 84 (100), 83 (8), 69 (45), 57 (10), 56 (12), 43 (8), 29 (11), 28 (30), 18 (19). $\mu_{\text{eff}} \sim 1.73 \mu_{\text{B}}$ (50–300 K). Anal. Calcd. for C₁₅H₂₀N₃O₅ (322.34): 55.9; H, 6.3; N, 13.0. Found: C, 55.7; H, 6.1; N, 12.8.

2-(3-(Ethoxycarbonyl)isoxazol-5-yl)-4,4,5,5-tetramethyl-4,5-dihydro-1H-imidazol-3-oxide 1-oxyl (11). To a stirred solution of **9** (170 mg, 0.94 mmol) and ethyl 2-chloro-2-(hydroxyimino)acetate (151 mg, 1.0 mmol) in dry Et₂O (15 ml) NEt₃ (0.1 ml) was added at 0 °C under argon atmosphere. The cooling bath was removed; the reaction mixture was stirred for 4 h and concentrated in vacuo. The obtained residue was put through a column with SiO₂ using ethyl acetate as the eluent. The blue-colored fraction was evaporated until dry under reduced pressure, the obtained residue was recrystallized from a mixture of *n*-heptane and CH₂Cl₂. Yield 140 mg (50%), blue needles, mp. 193–195 °C, *R*_f 0.73 (ethyl acetate). IR: ν = 3177, 2990, 2942, 1745, 1599, 1459, 1383, 1373, 1256, 1218, 1196, 1172, 1137, 1018, 934, 864, 834, 780, 623 cm⁻¹. $\mu_{\text{eff}} \sim 1.73 \mu_{\text{B}}$ (30–300 K). Anal. Calcd. for C₁₃H₁₈N₃O₅ (296.30): 52.7; H, 6.1; N, 14.2. Found: C, 53.0; H, 6.1; N, 14.4.

4,4,5,5-Tetramethyl-2-(1-(pyrrolidin-1-yl)but-3-ynyl)-4,5-dihydro-1H-imidazol-3-oxide 1-oxyl (12). To a stirred solution of enyne **2** (207 mg, 1.0 mmol) in toluene (20 ml) pyrrolidine (0.15 ml, 1.8 mmol) was added at 0 °C. The reaction mixture was stirred at room temperature for 24 h and concentrated in vacuo. The obtained residue was put through a column with SiO₂ using Et₂O as the eluent. The crimson-colored fraction was evaporated until dry under reduced pressure; the obtained residue was recrystallized from *n*-heptane with filtration. Yield 72 mg (26%), crimson crystals, mp 97–98 °C, *R*_f 0.20 (Et₂O). IR: ν = 3242, 2966, 2875, 2805, 2102, 1450, 1410, 1372, 1326, 1252, 1208, 1165, 1138, 933, 831, 725, 618, 541, 531, 461 cm⁻¹. HRMS, *m/z*: 278.1867 (M⁺, calcd. for C₁₅H₂₄N₃O₂ 278.1863). MS, *m/z* (%): 278 (M⁺, 1), 261 (2), 260 (2), 246 (3), 244 (4), 205 (2), 147 (2), 109 (7), 108 (100), 107 (4), 106 (6), 84 (3), 82 (2), 70 (2), 66 (4), 55 (4), 41 (4), 39 (2). Anal. Calcd. for C₁₅H₂₄N₃O₂ (278.37): C, 64.7; H, 8.7; N, 15.1. Found: C, 64.7; H, 8.7; N, 15.1.

2,2'-((1E,7E)-Octa-1,7-dien-3,5-diyne-1,8-diyl)bis(4,4,5,5-tetramethyl-4,5-dihydro-1H-imidazol-3-oxide 1-oxyl) (13). Through a mixture of **5** (30 mg, 0.15 mmol), CuCl (2 mg, 0.02 mmol), *N,N,N',N'*-tetramethylethylene-1,2-diamine (2 mg, 0.02 mmol) and acetone (3 ml) oxygen was bubbled at room temperature until **5** disappeared (TLC control). The reaction mixture was diluted with CHCl₃ (5 ml) and put onto a column with SiO₂ (1.5 × 15 cm) wetted with CHCl₃. The column was eluted with CHCl₃. The yellow-green fraction was diluted with *n*-heptane (5 ml) and evaporated in vacuo until residue formed which was filtered off and recrystallized from a mixture of ethyl acetate with *n*-heptane. Yield 15 mg (50%), bundles of thin

yellow-green crystals, R_f 0.68 (ethyl acetate); the crystals turn brown upon heating above 120–125 °C. IR: $\nu = 3053, 2982, 2938, 2597, 2353, 2310, 2180, 1808, 1581, 1451, 1432, 1415, 1387, 1372, 1308, 1264, 1243, 1212, 1165, 1137, 968, 860, 743, 616, 541, 477, 447, 421 \text{ cm}^{-1}$. UV/Vis (CHCl_3): $\lambda_{\text{max}} (\epsilon, \text{M}^{-1}\text{cm}^{-1}) = 269 (15000), 292 (14000), 330 \text{ sh. (23000)}, 346 (30000), 374 (37000), 403 (38000) \text{ nm}$. $\mu_{\text{eff}} \sim 2.45 \mu_B (100\text{--}300 \text{ K})$. Anal. Calcd. for $\text{C}_{18}\text{H}_{24}\text{N}_4\text{O}_4 (360.41)$: C, 64.1; H, 6.8; N, 13.6. Found: C, 63.8; H, 6.6; N, 13.5.

X-Ray structure determinations

Crystal data for compounds were collected on a Smart APEX CCD diffractometer using graphite-monochromated Mo- $K\alpha$ ($\lambda = 0.71073 \text{ \AA}$). The cell parameters were determined and refined by the least squares method for all reflections. The structures were solved by direct methods and refined by least squares procedures on F^2 . All non-hydrogen atoms were refined anisotropically. Positions of all hydrogen atoms were calculated geometrically and refined as riding on the respective carbon-bonded atoms. All structure solution and refinement calculations were performed with Bruker Shelxtl Version 6.12. The worst situation was with **13**, which forms very fine thread-like single crystals. As a result, we determined only the structure of the molecule, and only the unit cell parameters are given for this compound.

Compound (3a). $\text{C}_{22.5}\text{H}_{23}\text{ClN}_5\text{O}_2$; $FW = 430.90$; $T = 295 \text{ K}$; Monoclinic, $P2_1/n$; $a = 12.761(7)$, $b = 10.899(6)$, $c = 15.916(8) \text{ \AA}$; $\beta = 94.625(9)^\circ$; $V = 2206.4(19) \text{ \AA}^3$; $Z = 4$, $D_C = 1.297 \text{ g/cm}^3$; $\mu = 0.202 \text{ mm}^{-1}$; $2.13 < \theta < 27.49^\circ$; 13767 collected, 4942 unique, $R_{\text{int}} = 0.0851$; 339 parameters; $Goof = 0.808$; R indices for $I > 2\sigma$ $R_1 = 0.0529$, $wR_2 = 0.1202$; R indices (all data) $R_1 = 0.1216$, $wR_2 = 0.1440$.

Compound (4a). $\text{C}_{22}\text{H}_{22}\text{N}_5\text{O}$; $FW = 372.45$; $T = 240 \text{ K}$; Orthorhombic, $Pbca$; $a = 14.6206(12)$, $b = 14.6087(15)$, $c = 19.0240(12) \text{ \AA}$; $V = 4063.3(6) \text{ \AA}^3$; $Z = 8$, $D_C = 1.218 \text{ g/cm}^3$; $\mu = 0.078 \text{ mm}^{-1}$; $2.14 < \theta < 28.34^\circ$; 18015 collected, 4687 unique, $R_{\text{int}} = 0.0759$; 254 parameters; $Goof = 0.727$; R indices for $I > 2\sigma$ $R_1 = 0.0460$, $wR_2 = 0.1190$; R indices (all data) $R_1 = 0.1379$, $wR_2 = 0.1597$.

Compound (3b). $\text{C}_{24}\text{H}_{26}\text{N}_5\text{O}$; $FW = 400.5$; $T = 240 \text{ K}$; Monoclinic, $P2_1/n$; $a = 19.775(4)$, $b = 11.672(2)$, $c = 21.437(5) \text{ \AA}$; $\beta = 115.348(12)^\circ$; $V = 4471.5(17) \text{ \AA}^3$; $Z = 8$, $D_C = 1.190 \text{ g/cm}^3$; $\mu = 0.076 \text{ mm}^{-1}$; $2.04 < \theta < 28.46^\circ$; 33185 collected, 10795 unique, $R_{\text{int}} = 0.1145$; 542 parameters; $Goof = 1.000$; R indices for $I > 2\sigma$ $R_1 = 0.0722$, $wR_2 = 0.2063$; R indices (all data) $R_1 = 0.2703$, $wR_2 = 0.2792$.

Compound (5). $\text{C}_{11}\text{H}_{15}\text{N}_2\text{O}_2$; $FW = 207.25$; $T = 295 \text{ K}$; Orthorhombic, $Pna2_1$; $a = 19.553(2)$, $b = 9.1114(11)$, $c = 13.6744(19) \text{ \AA}$; $\beta = 109.277(11)^\circ$; $V = 2299.6(5) \text{ \AA}^3$; $Z = 8$, $D_C = 1.197 \text{ g/cm}^3$; $\mu = 0.084 \text{ mm}^{-1}$; $2.75 < \theta < 26.38^\circ$; 9351 collected, 2333 unique, $R_{\text{int}} = 0.0521$; 184 parameters; $Goof = 1.000$; R indices for $I > 2\sigma$ $R_1 = 0.0380$, $wR_2 = 0.0673$; R indices (all data) $R_1 = 0.0739$, $wR_2 = 0.0991$.

Compound (6a). $\text{C}_{12}\text{H}_{17}\text{N}_4\text{O}_2$; $FW = 249.30$; $T = 295 \text{ K}$; Monoclinic, $C2/c$; $a = 12.680(3)$, $b = 9.066(2)$, $c = 22.629(5) \text{ \AA}$; $V = 2601.2(10) \text{ \AA}^3$; $Z = 8$, $D_C = 1.273 \text{ g/cm}^3$; $\mu = 0.090 \text{ mm}^{-1}$; $1.80 < \theta < 27.04^\circ$; 7408 collected, 4017 unique, $R_{\text{int}} = 0.0349$; 333 parameters; $Goof = 0.877$; R indices for $I > 2\sigma$ $R_1 = 0.0537$, $wR_2 = 0.1244$; R indices (all data) $R_1 = 0.0995$, $wR_2 = 0.1411$.

Compound (6b). $C_{14}H_{21}N_4O_4$; $FW = 309.35$; $T = 240$ K; Monoclinic, $P2_1/c$; $a = 10.2311(5)$, $b = 10.1140(4)$, $c = 14.9675(7)$ Å; $\beta = 90.485(3)^\circ$; $V = 1548.74(12)$ Å³; $Z = 4$, $D_C = 1.327$ g/cm³; $\mu = 0.099$ mm⁻¹; $2.72 < \theta < 27.91^\circ$; 25066 collected, 3688 unique, $R_{int} = 0.0596$; 280 parameters; $Goof = 0.717$; R indices for $I > 2\sigma$ $R_1 = 0.0390$, $wR_2 = 0.0943$; R indices (all data) $R_1 = 0.0863$, $wR_2 = 0.1132$.

Compound (11). $C_{13}H_{18}N_3O_5$; $FW = 296.30$; $T = 240$ K; Monoclinic, $P2_1/n$; $a = 7.178(3)$, $b = 17.301(6)$, $c = 12.046(3)$ Å; $\beta = 98.32(2)^\circ$; $V = 1480.3(8)$ Å³; $Z = 4$, $D_C = 1.330$ g/cm³; $\mu = 0.103$ mm⁻¹; $2.07 < \theta < 28.42^\circ$; 11798 collected, 3550 unique, $R_{int} = 0.2119$; 191 parameters; $Goof = 0.946$; R indices for $I > 2\sigma$ $R_1 = 0.0590$, $wR_2 = 0.1142$; R indices (all data) $R_1 = 0.0968$, $wR_2 = 0.1636$.

Compound (13). $C_{16}H_{28}N_4O_4$; $FW = 340.42$; $T = 173$ K; Monoclinic, $P2_1/n$; $a = 9.7117(18)$, $b = 22.485(4)$, $c = 10.447(2)$ Å; $\beta = 103.44^\circ$; $V = 2218.8(7)$ Å³; $Z = 4$, $D_C = 1.019$ g/cm³.

Compound [(Cu(hfac)₂)₃(6c)₂]·C₇H₁₆. $C_{61}H_{56}Cu_3F_{36}N_4O_{16}$; $FW = 1975.72$; $T = 240$ K; Triclinic, $P-1$; $a = 11.4116(10)$, $b = 11.6299(10)$, $c = 16.8443(15)$ Å; $\alpha = 107.298(4)$, $\beta = 98.428(4)$, $\gamma = 106.055(3)^\circ$; $V = 1986.3(3)$ Å³; $Z = 1$, $D_C = 1.652$ g/cm³; $\mu = 0.943$ mm⁻¹; $1.92 < \theta < 32.29^\circ$; 47428 collected, 13446 unique, $R_{int} = 0.0422$; 682 parameters; $Goof = 0.941$; R indices for $I > 2\sigma$ $R_1 = 0.0343$, $wR_2 = 0.0906$; R indices (all data) $R_1 = 0.0609$, $wR_2 = 0.0976$.

Magnetic measurements

The magnetochemical measurements were performed on a MPMSXL SQUID magnetometer (Quantum Design) in the 2–300 K temperature range at a magnetic field strength $H = 5$ kOe. The molar magnetic susceptibility χ was calculated taking into account the atomic diamagnetism according to the Pascal additive scheme. In the paramagnetic region, the effective magnetic moment was calculated from the equation $\mu_{eff} = [(3k/N_A\beta^2) \chi T]^{1/2} \approx (8 \chi T)^{1/2}$, where k is the Boltzmann constant, N_A is Avogadro's number and β is the Bohr magneton.

Supplementary Information

Dependences of $\mu_{eff}(T)$ for the nitroxides **3a,b**, **4a,b**, **5**, **6b** and **13**, ESR spectra of **3b** and **4b** and the result of their modeling, molecular structures of **11** and [(Cu(hfac)₂)₃(**6c**)₂]·C₇H₁₆ are available as Supporting Information.

Crystallographic data for compounds have been deposited with the Cambridge Crystallographic Data Centre: CCDC Nos. 781679 (**11**), 781680 (**3a**), 781681 (**3b**), 781682 (**4a**), 781683 (**5**), 781684 (**6a**), 781685 (**6b**), 802867 [(Cu(hfac)₂)₃(**6c**)₂]·C₇H₁₆. This information can be obtained free of charge from The Director, CCDC, 12 Union Road, Cambridge, CB2 1EZ, UK (fax: +44-1223-336033; e-mail: deposit@ccdc.cam.ac.uk or <http://www.ccdc.cam.ac.uk>).

Acknowledgements

The financial support by Russian Foundation for Basic Research (grants 09-03-00091, 09-03-12108, 08-03-00025, 10-03-00756-a), U.S. Civilian Research and Development Foundation (REC-005), the Ministry of Science and Education (Grant for Leading Scientific Schools, Project NSh-65261.2010.3), Ural and Siberian Branches of the Russian Academy of Sciences is gratefully acknowledged.

References

1. Ullman, E. F.; Osiecki, J. H.; Boocock, D. G. B.; Darcy, R. *J. Am. Chem. Soc.* **1972**, *94*, 7049.
2. Tretyakov, E. V.; Ovcharenko V. I. *Russ. Chem. Rev.* **2009**, *78*, 971.
3. Boocock, D. G. B.; Darcy, R.; Ullman E. F. *J. Am. Chem. Soc.* **1968**, *21*, 5945.
4. (a) Leute, R. K.; Ullman, E. F. U.S. Patent 3 697 535, 1972. (b) Weiss, R.; Kraut, N.; Hampel, F. *J. Organomet. Chem.* **2001**, *617*, 473. (c) Fokin, S. V.; Romanenko, G. V.; Baumgarten, M.; Ovcharenko, V. I. *J. Struct. Chem.* **2003**, *44*, 864.
5. (a) Ovcharenko, V. I.; Chupakhin, O. N.; Kovalev, I. S.; Tretyakov, E. V.; Romanenko, G. V.; Stass, D. V. *Russ. Chem. Bull., Int. Ed.* **2008**, *57*, 2227. (b) Chupakhin, O. N.; Utepova, I. A.; Varaksin, M. V.; Tretyakov, E. V.; Romanenko, G. V.; Stass, D. V.; Ovcharenko, V. I. *J. Org. Chem.* **2009**, *74*, 2870.
6. Chupakhin, O. N.; Charushin, V. N.; van der Plas, H. *Nucleophilic Aromatic Substitution of Hydrogen*; Academic Press: New York, San Diego, 1994; p. 367.
7. Makosza, M.; Wojciechowski, K. *Chem. Rev.* **2004**, *104*, 2631.
8. Okusa, G.; Kumagai, M.; Itai, T. *Chem. Pharm. Bull.* **1969**, *17*, 2502.
9. Igeta, H.; Tsuchiya, T.; Nakai, T. *Tetrahedron Lett.* **1969**, 2667.
10. (a) Mitsunashi, K.; Takayanagi, H.; Matsuno, S.; Tanaka, K. *J. Heterocycl. Chem.* **1982**, *19*, 1389. (b) Yang, J.; Gharagozloo, P.; Yao, J.; Ilyin, V. I.; Carter, R. B.; Nguyen, P.; Robledo, S.; Woodward, R. M.; Hogenkamp, D. J. *J. Med. Chem.* **2004**, *47*, 1547.
11. Werner, E. A. *J. Chem. Soc.* **1919**, *115*, 1093.
12. Campbell, M. M.; Coaford, N. D. P.; Rae, D. R.; Sainsbury, M. *J. Chem. Soc., Perkin Trans. I* **1991**, 765.
13. Tretyakov, E.; Romanenko, G.; Podoplelov, A.; Ovcharenko, V. *Eur. J. Org. Chem.* **2006**, 2695.
14. (a) Tretyakov, E.; Romanenko, G.; Ikorskii, V.; Stass, D.; Vasiliev, V.; Demina, M.; Mareev, A.; Medvedeva, A.; Gorelik, E.; Ovcharenko, V. *Eur. J. Org. Chem.* **2007**, 3639. (b) Tretyakov, E.; Tolstikov, S.; Mareev, A.; Medvedeva, A.; Romanenko, G.; Stass, D.; Bogomyakov, A.; Ovcharenko, V. *Eur. J. Org. Chem.* **2009**, 2548.
15. Eglinton, G.; Galbraith, A. R. *J. Chem. Soc.* **1959**, 889.

16. Hay, A. S. *J. Org. Chem.* **1962**, 27, 3320.
17. *Org. Synth.* **1993**; *Coll. Vol.* 8, 63. *Org. Synth.* **1987**, 65, 52.
18. Allen, F. H.; Kennard, O.; Watson, D. G.; Brammer, L.; Orpen, A. G.; Taylor, R. *J. Chem. Soc., Perkin Trans. 2* **1987**, S1.
19. Bleaney, B.; Bowers, K. D. *Proc. Roy. Soc.* **1952**, A214, 451.
20. Ginsberg, A. P.; Lines, M. E. *Inorg. Chem.* **1972**, 11, 2289.
21. (a) Bolton, J. R.; Carrington, A. *Mol. Phys.* **1962**, 5, 161. (b) Freed, J. H.; Fraenkel, G. K. *J. Chem. Phys.* **1962**, 37, 1156.
22. Yamanaka, H.; Sakamoto, T.; Niitsuma, S. *Heterocycles* **1990**, 31, 923.
23. (a) Ovcharenko, V. I.; Fokin, S. V.; Korobkov, I. V.; Rey P. *Russ. Chem. Bull.* **1999**, 48, 1519 (Engl. Transl.). (b) Hirel, C.; Vostrikova, K. E.; Pecaut, J.; Ovcharenko, V. I.; Rey. P. *Chem. Eur. J.* **2001**, 7, 2007.
24. Edwards, L.; Slassi, A.; Isaac, M.; McLeod, D. U.S. Patent 20 070 037 820, 2007.
25. Sviridenko, F. B.; Stass, D. V.; Kobzeva, T. V.; Tretyakov, E. V.; Klyatskaya, S. V.; Mshvidobadze, E. V.; Vasilevsky, S. F.; Molin, Yu. N. *J. Am. Chem. Soc.* **2004**, 126, 2807.
26. Bennett, G. B. U.S. Patent 3 963 713, 1976.
27. (a) Atkinson, C. M.; Cossey H. D. *J. Chem. Soc.* **1962**, 1805. (b) Saraswathi, T. V.; Srinivasan, V. R. *Tetrahedron* **1977**, 33, 1043.